Adsorption-controlled molecular-beam epitaxial growth of $BiFeO_3$

J. F. Ihlefeld, A. Kumar, V. Gopalan, and D. G. Schlom[a)]
Department of Materials Science and Engineering, Pennsylvania State University, University Park, Pennsylvania 16802-5005

Y. B. Chen and X. Q. Pan
Department of Materials Science and Engineering, University of Michigan, Ann Arbor, Michigan 48019

T. Heeg and J. Schubert
Institute of Bio- and Nano-Systems (IBN1-IT), Research Centre Jülich, D-52425 Jülich, Germany

X. Ke and P. Schiffer
Department of Physics, The Pennsylvania State University, University Park, Pennsylvania 16802

J. Orenstein
Department of Physics, University of California, Berkeley, California 94720-1760 and Lawrence Berkeley National Laboratory, Berkeley, California 94720-7300

L. W. Martin, Y. H. Chu, and R. Ramesh
Department of Materials Science and Engineering and Department of Physics, University of California, Berkeley, California 94720-1760

(Received 24 April 2007; accepted 10 July 2007; published online 17 August 2007)

$BiFeO_3$ thin films have been deposited on (111) $SrTiO_3$ single crystal substrates by reactive molecular-beam epitaxy in an adsorption-controlled growth regime. This is achieved by supplying a bismuth overpressure and utilizing the differential vapor pressures between bismuth oxides and $BiFeO_3$ to control stoichiometry. Four-circle x-ray diffraction reveals phase-pure, untwinned, epitaxial, (0001)-oriented films with rocking curve full width at half maximum values as narrow as 25 arc sec (0.007°). Second harmonic generation polar plots combined with diffraction establish the crystallographic point group of these untwinned epitaxial films to be $3m$ at room temperature.
 [DOI: 10.1063/1.2767771]

A popular multiferroic that displays both ferroelectric and antiferromagnetic behaviors at room temperature is $BiFeO_3$. Bulk bismuth ferrite at room temperature possesses rhombohedral symmetry, space group $R3c$ (point group $3m$), with lattice constants $a=5.5785$ Å and $c=13.8688$ Å for hexagonal axes of reference (used throughout this letter).[1] In thin films, this material possesses a spontaneous electric polarization (P_s) of $\sim 100\ \mu C/cm^2$, the highest of any known ferroelectric.[2] This is an order of magnitude greater than that originally reported for bulk $BiFeO_3$ samples, which gave rise to a flurry of work exploring the film symmetry to elucidate any structure property relations.[2–7] These studies established that 200 nm thick epitaxial $BiFeO_3$ films grown on $(001)_p$ and $(011)_p$ perovskite substrates (where p subscript denotes pseudocubic indices) possess a slight monoclinic distortion, while 200 nm thick films grown on $(111)_p$-oriented substrates are rhombohedral.[2,3,5–7] Recent measurements on bulk $BiFeO_3$ indicates that the high P_s value is intrinsic to rhombohedral $BiFeO_3$.[8]

As the polar axis has four possible variants along the pseudocubic $\langle 111\rangle_p$ directions, only one of which is the [0001]$BiFeO_3$ polar axis, knowledge and control of domain structure are crucial in interpreting material property measurements development. Here, we show that films grown on (111) $SrTiO_3$ substrates are untwinned with the polar axis perpendicular to the plane of the substrate.

To unambiguously probe fundamental material properties, it is desirable to have films with high crystalline quality to minimize extrinsic effects arising from defects. Films deposited by reactive molecular-beam epitaxy (MBE) are especially well suited for this. While epitaxial bismuth ferrite, has been grown by chemical vapor deposition,[9] pulsed-laser deposition (PLD),[6,10] and rf sputtering,[11] there exist limited reports of growth by MBE.[12] In this letter, we demonstrate the epitaxial growth of $BiFeO_3$ by MBE using adsorption-controlled growth and discuss the resulting crystal quality, film orientation, and symmetry.

In addition to compound semiconductor films, adsorption-controlled film growth has previously been demonstrated for several bismuth- and lead-containing ferroelectric oxides.[13–16] The adsorption-controlled growth regime is enabled by a differential vapor pressure between the desired phase, $BiFeO_3$, and all other binary bismuth oxide phases Bi_xO_y. Within a window of substrate temperature and bismuth overpressure, phase-pure films of $BiFeO_3$ can be grown with the excess bismuth oxide phases desorbing. As the free energy of $BiFeO_3$ and other relevant species are unknown, the growth window for the adsorption-controlled growth of $BiFeO_3$ was established experimentally.

The films were grown in a Veeco 930 MBE system described elsewhere.[17] Single crystalline $SrTiO_3$ substrates oriented within ±0.1° of (111) were used. $BiFeO_3$ films were deposited at temperatures between 330 and 420 °C with Bi to Fe flux ratios ranging from 4:1 to 8:1 as measured by a quartz crystal microbalance with doses calibrated by Rutherford backscattering spectrometry (RBS). The substrate temperatures are significantly lower than commonly used by other techniques to grow $BiFeO_3$ films. As these tempera-

[a)]Electronic mail: schlom@ems.psu.edu

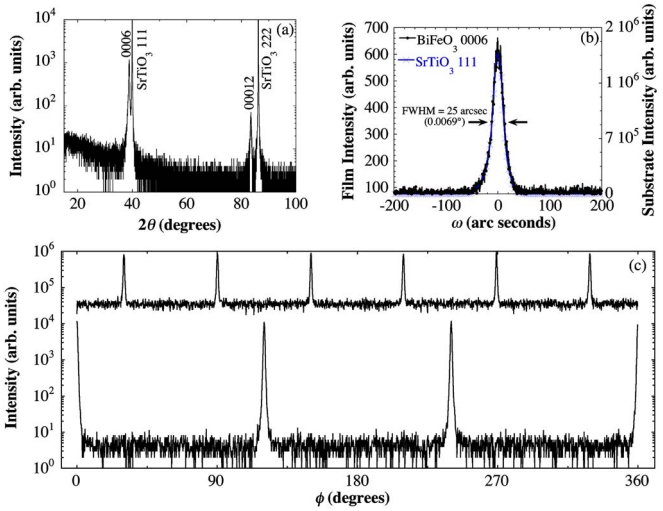

FIG. 1. (Color online) (a) θ-2θ x-ray diffraction pattern from a 35 nm thick (0001)-oriented $BiFeO_3$ on (111) $SrTiO_3$ grown at approximately 400 °C with a Bi:Ti ratio of 7:1. (b) Superimposed rocking curves of the 0006 $BiFeO_3$ film and 111 $SrTiO_3$ substrate peaks. (c) Azimuthal ϕ scans of the $2\bar{1}\bar{1}3$ (top) (χ=58.9°) and $10\bar{1}2$ (bottom) (χ=55.1°) $BiFeO_3$ diffraction peaks. χ=90° aligns the diffraction vector to be perpendicular to the plane of the substrate. ϕ=0° is aligned to be parallel to the $[1\bar{1}0]$ in-plane projection of the (111) $SrTiO_3$ substrate. Together these XRD scans show that the $BiFeO_3$ film is epitaxial, untwinned, and oriented with (0001) $BiFeO_3 \| (111)$ $SrTiO_3$ and $[2\bar{1}\bar{1}0] \| [1\bar{1}0]$ $SrTiO_3$.

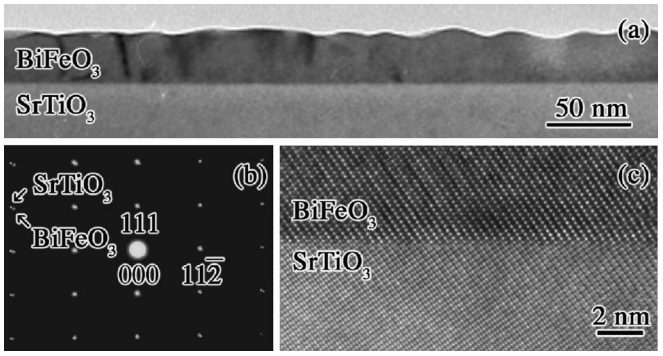

FIG. 2. (a) Bright-field TEM image of the same film whose XRD is shown in Fig. 1. (b) Selected-area electron diffraction from region covering the film and the substrate. Reflections from the $SrTiO_3$ substrate are indexed. (c) HRTEM image of the film/substrate interface.

tures are too low for conventional visible optical pyrometers, the substrate temperature was determined by the temperature dependence of the $SrTiO_3$ band edge.[18,19] An ozone/oxygen mixture (~10% ozone) was supplied continuously during growth at a 1×10^{-6} Torr background pressure. The films were grown in a similar manner to previous adsorption controlled oxides[14–16] with the volatile bismuth and oxygen components supplied continuously and the nonvolatile component (iron) supplied in doses corresponding to individual iron monolayers making up the BiO_3–Fe–BiO_3–Fe–⋯ stacking sequence along [0001] of the $BiFeO_3$ structure.

After heating the (111) $SrTiO_3$ substrate to growth temperature, ozone and bismuth were introduced. Due to the high vapor pressure of Bi_2O_3, the substrate could be exposed to Bi and ozone for arbitrary long periods prior to the initiation of $BiFeO_3$ growth. $BiFeO_3$ growth was initiated by opening the iron shutter. The $BiFeO_3$ growth was three-dimensional as can be expected given the high bond density of the $(111)_p$ pseudocubic faces, similar to what has been observed for other heteroepitaxial oxide films when an orientation with a high surface energy is attempted.[20,21]

A 35 nm thick $BiFeO_3$ film on (111) $SrTiO_3$ grown at a substrate temperature of 400 °C was characterized by XRD. The θ-2θ scan in Fig. 1(a) is consistent with the growth of phase-pure (0001)-oriented $BiFeO_3$. Rocking curves of the 0006 film peak [shown in Fig. 1(b)] had a full width at half maximum (FWHM) of 25 arc sec (0.007°). This FWHM is the same as the underlying $SrTiO_3$ substrate, indicating that the film crystallinity is substrate limited. This low rocking curve value marks a substantial improvement over $BiFeO_3$ films grown by all other techniques.[11] To better establish the symmetry of the $BiFeO_3$ film, a ϕ scan of the $2\bar{1}\bar{1}3$ family of peaks ($2\bar{1}\bar{1}3$, $1\bar{2}13$, $\bar{1}\bar{1}23$, $\bar{2}113$, $\bar{1}2\bar{1}3$, and $1\bar{1}23$) was made. Cubic or tetragonal $BiFeO_3$ would not exhibit diffraction at these peak positions.[11] As Fig. 1(c) shows, however, such peaks are clearly present, consistent with the rhombohedral $3m$ point group symmetry of bulk $BiFeO_3$.

The six peaks seen in the ϕ scan of Fig. 1(c) indicate that the $BiFeO_3$ film is epitaxial with orientation relationship (0001) $BiFeO_3 \| (111)$ $SrTiO_3$ and $[2\bar{1}\bar{1}0] \| [1\bar{1}0]$ $SrTiO_3$. To see whether it contains in-plane rotational twinning, a ϕ scan of a $BiFeO_3$ peak that would only show three peaks in an untwinned single crystal was made. The $10\bar{1}2$ $BiFeO_3$ family of peaks ($10\bar{1}2$, $0\bar{1}12$, and $\bar{1}102$) was selected because it is intense and unambiguous (does not overlap with other peaks of the film or substrate). The resulting ϕ scan [Fig. 1(c)] contains just three peaks, indicative of a single in-plane orientation.

Another type of twinning that an epitaxial $BiFeO_3$ film could contain is for other $(111)_p$ pseudocubic $BiFeO_3$ planes to be parallel to the (111) plane of the $SrTiO_3$ substrate. Rhombohedral $BiFeO_3$ contains four different $(111)_p$ pseudocubic planes: (0001), $(2\bar{1}\bar{1}3)$, $(\bar{1}\bar{1}23)$, and $(\bar{1}2\bar{1}3)$. The spontaneous polarization, however, only lies perpendicular to *one* of these planes, i.e., (0001). X-ray diffraction scans were performed to see if any of these other planes lie in the vicinity of being parallel to the (111) $SrTiO_3$ substrate surface. No peaks could be distinguished from the background intensity level. Consideration of the intensity of the 0006 peak observed and the calculated intensity ratio to the $BiFeO_3$ peaks not seen (e.g., the $4\bar{2}\bar{2}6$ peak) allows us to conclude that macroscopically the film is untwinned and at least 99.8% (0001) or $(000\bar{1})$ oriented.

The TEM images in Fig. 2 show that the interface between the $BiFeO_3$ thin films and the substrate is atomically sharp, although the film surface is rough. RBS indicates a Bi:Fe stoichiometry of 0.92 (±0.03):1 and a minimum channeling yield χ_{min}=8%. The bismuth deficiency suggests a large single-phase field for $BiFeO_3$, similar to that of $PbTiO_3$ (Refs. 22 and 23) and significantly wider than semiconductor materials, e.g., GaAs.[24,25]

Second harmonic generation (SHG) was employed to further assess the crystal symmetry. SHG involves the conversion of light (electric field E^{ω}) at a frequency ω into an optical signal at a frequency 2ω by a nonlinear medium, through the creation of a nonlinear polarization $P^{2\omega} \propto d_{ijk}E^{\omega}E^{\omega}$. Here, d_{ijk} refers to the nonlinear optical coefficient tensor. The light source for SHG was a Ti:sapphire laser with a pulse width of 140 fs, a repetition rate of 1 kHz,

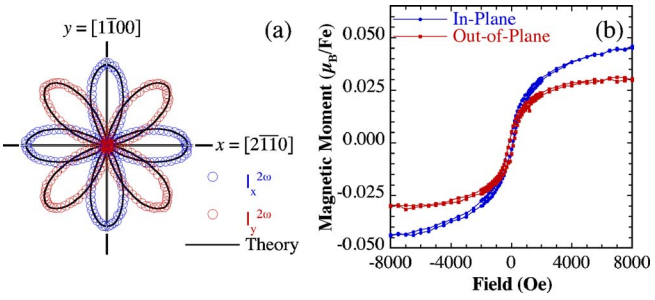

FIG. 3. (Color online) (a) Polar plots of SHG intensities $I_x^{2\omega}$ and $I_y^{2\omega}$ from the same film studied in Figs. 1 and 2 in normal incidence as a function of the angle θ from the y axis theoretical values obtained from Eqs. (1) and (2). (b) Magnetic hysteresis loops from the same film measured parallel and perpendicular to the (0001) $BiFeO_3$ plane.

and a wavelength of 800 nm. A fundamental wave of 800 nm was incident from the substrate side in normal geometry. Its polarization direction, at an angle θ from the y axis, was rotated continuously within the plane of the film. The intensity $I_j^{2\omega}$ of the output SHG signal at 400 nm wavelength from the film was detected along either $j=x[2\bar{1}\bar{1}0]$, $y[1\bar{1}00]$ directions of the film by a photomultiplier tube. The resulting polar plots of the SHG intensity at room temperature are shown in Fig. 3(a). A reference study of a bare (111) $SrTiO_3$ substrate without any film yielded no SHG intensity within the detection limits. Excellent theoretical fits to this data are given by the following equations:

$$I_x = K_1 \sin^2 2\theta, \tag{1}$$

$$I_y = K_1 \cos^2 2\theta. \tag{2}$$

The constant $K_1 \propto (A_{z+} - A_{z-})^2 d_{22}^2$, where d_{22} refers to the nonlinear optical coefficient and A_{z+} and A_{z-} represent the area fractions of the domains with polarization along the [0001] and $[000\bar{1}]$ film axes, respectively. If the SHG signal is dominated by coupling to the crystallographic lattice, this reduces the possible point group of the film to $3m$. If the SHG is dominated by magnetism, then the possible magnetic point groups are $32'$, $3m'$, and $\bar{3}m'$. Since the material is ferroelectric and cannot have inversion symmetry, $\bar{3}m'$ can be eliminated. Note that these are symmetries of the measured SHG property, and the actual magnetic structure itself is allowed to have a lower subgroup symmetry (such as $2'$, m, or m'). Resolving these will be reported separately.

Room temperature magnetic measurements, Fig. 3(b), reveal saturation magnetizations of approximately 0.04 and 0.03 Bohr magnetons per iron atom in plane and out of plane, respectively, the absolute values of which are consistent with films grown by other techniques.[10,26] Although theoretical predictions indicate the magnetism to be in the (0001) plane with a significant magnetic anisotropy of about 2 meV/unit cell,[27] these magnetic measurements indicate more of a mixed state of anisotropy. These observations are also similar to that obtained in films deposited by PLD. Due to the relatively small magnitude of the absolute magnetic moment, caution is required in terms of magnetic measurements; we note that these absolute magnitudes are well within the range of the SQUID system (1×10^{-8} emu) with RSO attachment. It thus suggests that further critical evaluation of the nature of the antiferromagnetic order and the canted moment might be required, especially in thin films that are constrained by a substrate.

This work was supported by the Office of Naval Research through Grant No. N00014-04-1-0426 monitored by Colin Wood, and by the NSF through Grant Nos. DMR-0213623, DMR-0122638, DMR-0507146, DMR-0512165, and DMR-0349632.

[1] F. Kubel and H. Schmid, Acta Crystallogr., Sect. B: Struct. Sci. **B46**, 698 (1990).
[2] J. F. Li, J. L. Wang, M. Wuttig, R. Ramesh, N. Wang, B. Ruette, A. P. Pyatakov, A. K. Zvezdin, and D. Viehland, Appl. Phys. Lett. **84**, 5261 (2004).
[3] F. M. Bai, J. L. Wang, M. Wuttig, J. F. Li, N. G. Wang, A. P. Pyatakov, A. K. Zvezdin, L. E. Cross, and D. Viehland, Appl. Phys. Lett. **86**, 032511 (2005).
[4] X. D. Qi, M. Wei, Y. Lin, Q. X. Jia, D. Zhi, J. Dho, M. G. Blamire, and J. L. MacManus-Driscoll, Appl. Phys. Lett. **86**, 071913 (2005).
[5] K. Saito, A. Ulyanenkov, V. Grossmann, H. Ress, L. Bruegemann, H. Ohta, T. Kurosawa, S. Ueki, and H. Funakubo, Jpn. J. Appl. Phys., Part 1 **45**, 7311 (2006).
[6] J. Wang, J. B. Neaton, H. Zheng, V. Nagarajan, S. B. Ogale, B. Liu, D. Viehland, V. Vaithyanathan, D. G. Schlom, U. V. Waghmare, N. A. Spaldin, K. M. Rabe, M. Wuttig, and R. Ramesh, Science **299**, 1719 (2003).
[7] G. Y. Xu, H. Hiraka, G. Shirane, J. F. Li, J. L. Wang, and D. Viehland, Appl. Phys. Lett. **86**, 182905 (2005).
[8] V. V. Shvartsman, W. Kleemann, R. Haumont, and J. Kreisel, Appl. Phys. Lett. **90**, 172115 (2007).
[9] S. Y. Yang, F. Zavaliche, L. Mohaddes-Ardabili, V. Vaithyanathan, D. G. Schlom, Y. J. Lee, Y. H. Chu, M. P. Cruz, Q. Zhan, T. Zhao, and R. Ramesh, Appl. Phys. Lett. **87**, 102903 (2005).
[10] H. Bea, M. Bibes, A. Barthelemy, K. Bouzehouane, E. Jacquet, A. Khodan, J. P. Contour, S. Fusil, F. Wyczisk, A. Forget, D. Lebeugle, D. Colson, and M. Viret, Appl. Phys. Lett. **87**, 072508 (2005).
[11] R. R. Das, D. M. Kim, S. H. Baek, C. B. Eom, F. Zavaliche, S. Y. Yang, R. Ramesh, Y. B. Chen, X. Q. Pan, X. Ke, M. S. Rzchowski, and S. K. Streiffer, Appl. Phys. Lett. **88**, 242904 (2006).
[12] J. Kabelac, S. Ghosh, P. S. Dobal, and R. Katiyar, J. Vac. Sci. Technol. B **25**, 1049 (2007).
[13] C. D. Theis, J. Yeh, D. G. Schlom, M. E. Hawley, and G. W. Brown, Thin Solid Films **325**, 107 (1998).
[14] C. D. Theis, J. Yeh, D. G. Schlom, M. E. Hawley, G. W. Brown, J. C. Jiang, and X. Q. Pan, Appl. Phys. Lett. **72**, 2817 (1998).
[15] S. Migita, H. Ota, H. Fujino, Y. Kasai, and S. Sakai, J. Cryst. Growth **200**, 161 (1999).
[16] D. G. Schlom, J. H. Haeni, J. Lettieri, C. D. Theis, W. Tian, J. C. Jiang, and X. Q. Pan, Mater. Sci. Eng., B **87**, 282 (2001).
[17] C. D. Theis and D. G. Schlom, J. Cryst. Growth **174**, 473 (1997).
[18] BANDIT, k-Space Associates, Ann Arbor, MI.
[19] E. S. Hellman and J. S. Harris, J. Cryst. Growth **81**, 38 (1987).
[20] H. S. Craft, J. F. Ihlefeld, M. D. Losego, R. Collazo, Z. Sitar, and J. P. Maria, Appl. Phys. Lett. **88**, 212906 (2006).
[21] W. Tian, V. Vaithyanathan, D. G. Schlom, Q. Zhan, S. Y. Yang, Y. H. Chu, and R. Ramesh, Appl. Phys. Lett. **90**, 172908 (2007).
[22] M. A. Eisa, M. F. Abadir, and A. M. Gadalla, Trans. J. Br. Ceram. Soc. **79**, 100 (1980).
[23] R. L. Holman, Ferroelectrics **14**, 675 (1976).
[24] A. I. Ivashchenko, F. Y. Kopanskaya, and G. S. Kuzmenko, J. Phys. Chem. Solids **45**, 871 (1984).
[25] S. Shirasaki, Solid State Commun. **9**, 1217 (1971).
[26] T. Zhao, A. Scholl, F. Zavaliche, K. Lee, M. Barry, A. Doran, M. P. Cruz, Y. H. Chu, C. Ederer, N. A. Spaldin, R. R. Das, D. M. Kim, S. H. Baek, C. B. Eom, and R. Ramesh, Nat. Mater. **5**, 823 (2006).
[27] C. Ederer and N. A. Spaldin, Phys. Rev. B **71**, 060401 (2005).